

# Gauge Mediated Supersymmetry Signals at the Tevatron Involving $\tau$ Leptons

B. Dutta<sup>1,a</sup>, D.J. Muller<sup>2</sup> and S. Nandi<sup>2,a</sup>

<sup>1</sup>*Institute of Theoretical Physics, University of Oregon, Eugene, OR 97403*

<sup>2</sup>*Department of Physics, Oklahoma State University, Stillwater, OK 74078*

<sup>a</sup> *Fermilab, P.O. Box 500, Batavia, IL 60510*

(July 1, 2021)

## Abstract

We consider the phenomenology of GMSB models where the lighter stau is the next to lightest supersymmetric particle. In this situation the dominant signals for supersymmetry at the Tevatron are events where two or three high  $p_T$   $\tau$  leptons accompanied by large missing transverse energy are produced. This leads to signatures that are very different from the photonic signals for GMSB (where the lightest neutralino is the NLSP) and the dilepton and trilepton signals in the usual supergravity models (involving  $e$  and/or  $\mu$  only) that have been investigated extensively. We find that the inclusive 2  $\tau$ -jet signature could be observable at the Tevatron Run II, while the inclusive 3  $\tau$ -jet signature could be important at Run III.

## I. INTRODUCTION

Supersymmetry (SUSY) has been the focus of a great deal of experimental effort due to the requirement that the superparticles have masses of  $\mathcal{O}(1)$  TeV or less in order to solve the hierarchy problem. Thus there exists the possibility of producing SUSY particles at present and the next generation of colliders. The phenomenology of such production depends on the nature of the supersymmetry breaking. In typical theories of SUSY breaking, the effects of this breaking, which occurs in a “hidden sector”, are communicated to the “visible sector” (which includes the usual particles and their superpartners) by a “messenger sector”. Searches for SUSY have mostly been inspired by gravity mediated SUSY breaking theories. In these theories, the lightest neutralino is usually the lightest supersymmetric particle (LSP). If R-parity is conserved, the LSP is stable and the decay chains of all other SUSY particles must eventually produce it. The LSP leaves the detector undetected thereby making large missing transverse energy ( $\cancel{E}_T$ ) an important part of the signature for SUSY. In spite of extensive experimental searches, so far no experimental evidence for SUSY has been found at the Tevatron [1] or at LEP [2] except for one possible  $e^+e^-\gamma\gamma$  plus  $\cancel{E}_T$  event at the Tevatron [3].

Recently, gauge mediated SUSY breaking (GMSB) models have become very popular [4–6]. The defining characteristic of GMSB models is that the messenger particles interact with visible sector particles via gauge interactions. In these theories, the gravitino is the LSP. Most phenomenological studies and experimental searches that have used GMSB as a framework have taken the next to lightest SUSY particle (NLSP) to be the lightest neutralino. When this is the case, the  $\chi_1^0$  decays to a photon and a gravitino ( $\tilde{G}$ ). If this decay takes place within the detector, the signal involves high  $p_T$  photons accompanied by large  $\cancel{E}_T$  [7]. For much of the parameter space, however, the lighter of the two scalar staus is the NLSP. In this case, the decays of SUSY particles produce the  $\tilde{\tau}_1$  which subsequently decays to a  $\tau$  and a gravitino. If the  $\tilde{\tau}_1$  decays occur within the detector, signatures for SUSY production will then generally include  $\tau$  leptons from the  $\tilde{\tau}_1$  decays and  $\cancel{E}_T$  due to the stable gravitinos and neutrinos leaving the detector.

It was proposed [8] that GMSB models where the  $\tilde{\tau}_1$  is the NLSP can lead to unusual and distinguishing signatures for gaugino production. At the Tevatron, these signals arise from chargino pair production ( $\chi_1^+\chi_1^-$ ) and from the production of the chargino with the second neutralino ( $\chi_1^\pm\chi_2^0$ ). The subsequent decays involve multiple high  $p_T$   $\tau$  leptons and possibly substantial  $\cancel{E}_T$ . The purpose of this paper is to analyze in detail the signals for these decay modes at the Tevatron. In particular, we seek to determine the production rates for various distinguishing final states, the  $E_T$  spectrum of the  $\tau$  jets, and the  $\cancel{E}_T$  distribution for the events.

## II. MASS SPECTRUM AND PRODUCTION MECHANISMS

Since the observed signal depends on the masses of the sparticles, we first begin by describing the model and the corresponding mass spectrum. In our model, the messenger sector consists of some number of multiplets that are  $\bar{5} + 5$  representations of SU(5). They couple to a chiral superfield  $S$  in the hidden sector whose scalar component has a vacuum expectation value (VEV)  $\langle s \rangle$  and whose auxiliary component has a VEV  $\langle F_s \rangle$ . By imposing

the requirement that the electroweak (EW) symmetry is broken radiatively, the particle spectrum and the mixing angles depend on five parameters:  $M$ ,  $\Lambda$ ,  $n$ ,  $\tan\beta$ , and the sign of  $\mu$ .  $M$  is the messenger scale.  $\Lambda$  is equal to  $\langle F_s \rangle / \langle s \rangle$  and is related to the SUSY breaking scale. The parameter  $n$  is dictated by the choice of the vector-like messenger sector and can take the values 1, 2, 3, or 4 to satisfy the perturbative unification constraint. The definition of  $\tan\beta$  is taken as  $\tan\beta \equiv v_2/v_1$  where  $v_2$  is the VEV for the up-type ( $H_u$ ) Higgs doublet and  $v_1$  is the VEV for the down-type ( $H_d$ ) Higgs doublet. The parameter  $\mu$  is the coefficient in the bilinear term,  $\mu H_u H_d$ , in the superpotential. Constraints coming from  $b \rightarrow s\gamma$  strongly favor negative values for  $\mu$  [9] and, in the cases considered in this work,  $\mu$  is taken to be negative. Demanding that the EW symmetry be broken radiatively fixes the magnitude of  $\mu$  and the parameter  $B$  (from the  $B\mu H_u H_d$  term in the scalar potential) in terms of the other parameters of the theory.

The soft SUSY breaking gaugino and scalar masses at the messenger scale are given by [4,10]

$$\tilde{M}_i(M) = n g \left( \frac{\Lambda}{M} \right) \frac{\alpha_i(M)}{4\pi} \Lambda \quad (1)$$

and

$$\tilde{m}^2(M) = 2 n f \left( \frac{\Lambda}{M} \right) \sum_{i=1}^3 k_i C_i \left( \frac{\alpha_i(M)}{4\pi} \right)^2 \Lambda^2 \quad (2)$$

where the  $\alpha_i$  are the three SM gauge couplings and  $k_i = 1, 1$ , and  $3/5$  for SU(3), SU(2), and U(1), respectively. The  $C_i$  are zero for gauge singlets and are  $4/3, 3/4$ , and  $(Y/2)^2$  for the fundamental representations of SU(3), SU(2), and U(1), respectively (with  $Y$  given by  $Q = I_3 + Y/2$ ).  $g(x)$  and  $f(x)$  are messenger scale threshold functions. We calculate the sparticle masses at the scale  $M$  using Eqs. (1) and (2) and run these to the electroweak scale using the appropriate RGE's [11].  $\mu^2$  is calculated by minimizing the 1 loop corrected Higgs potential [11].

The decay chain and hence the signature for the events depends on the particles initially produced as well as the hierarchy of the masses. Given the current lower bounds on squark and gluino masses, the production of strongly interacting sparticles is probably not a viable search modes for SUSY at the Tevatron Run II. A more likely mechanism for producing SUSY particles is via EW gaugino production. At the tevatron, chargino pair ( $\chi_1^+ \chi_1^-$ ) production takes place through s-channel  $Z$  and  $\gamma$  exchange and  $\chi_2^0 \chi_1^\pm$  production is through s-channel  $W$  exchange. Squark exchange via the t-channel also contributes to both processes, but the contributions are expected to be negligible since the squark masses are large in GMSB models. The production of  $\chi_1^0 \chi_1^\pm$  is suppressed due to the smallness of the coupling involved.

Since SUSY breaking is communicated to the visible sector by gauge interactions, the mass differences between the superparticles depend on the their gauge interactions. This creates a hierarchy in mass between electroweak and strongly interacting sparticles. Eq. (1) shows that the gluino is more massive than charginos and neutralinos, while Eq. (2) shows that squarks are considerably more massive than sleptons. Given this hierarchy of particle masses, there are roughly four possible cases to consider for EW gaugino production:

$$\textbf{Case 1: } m_{\tilde{\nu}} > M_{\chi_2^0} \gtrsim M_{\chi_1^\pm} > m_{\tilde{e}_1, \tilde{\mu}_1} > M_{\chi_1^0} > m_{\tilde{\tau}_1}$$

$$\textbf{Case 2: } M_{\chi_2^0} \gtrsim M_{\chi_1^\pm} > m_{\tilde{\nu}} > M_{\chi_1^0} > m_{\tilde{e}_1, \tilde{\mu}_1} > m_{\tilde{\tau}_1}$$

$$\textbf{Case 3: } M_{\chi_2^0} \gtrsim M_{\chi_1^\pm} > m_{\tilde{\nu}} > m_{\tilde{e}_1, \tilde{\mu}_1} > M_{\chi_1^0} > m_{\tilde{\tau}_1}$$

$$\textbf{Case 4: } m_{\tilde{\nu}} > M_{\chi_2^0} \gtrsim M_{\chi_1^\pm} > M_{\chi_1^0} > m_{\tilde{e}_1, \tilde{\mu}_1} > m_{\tilde{\tau}_1}$$

The three sneutrino masses are nearly the same. The lighter of the selectrons and smuons are essentially right handed and have the same mass. Also, for all the parameter points we considered,  $\chi_1^\pm$  and  $\chi_2^0$  are nearly degenerate.

The possible final states configurations at the Tevatron depend on the sparticle spectrum, but they will have certain aspects in common. Since the  $\tilde{\tau}_1$  is the NLSP, the various possible decays modes will (usually) produce at least two  $\tau$  leptons arising from the decays of the  $\tilde{\tau}_1$ 's. In addition, there can also be large  $\cancel{E}_T$  due to the stable gravitinos and neutrinos escaping detection.

### III. ANALYSIS AND RESULTS

We now give a detailed analysis of the possible Tevatron signatures for gaugino production in the context of GMSB models where the lightest stau is the NLSP. As mentioned above, the production of SUSY particles in these models leads to the production of copious quantities of  $\tau$  leptons. Since the lightest chargino is mostly wino, it couples mainly to left-handed sfermions. Thus, for the examples considered here, the dominant decay mode of the chargino is typically  $\chi_1^\pm \rightarrow \tilde{\tau}_1 \nu_\tau$  due to the significant mixing of the left and right handed staus and the low mass of the  $\tilde{\tau}_1$ . With the subsequent decay  $\tilde{\tau}_1 \rightarrow \tau \tilde{G}$ , the expectation is that there are typically two  $\tau$  leptons produced in chargino pair production. Similarly,  $\chi_2^0 \rightarrow \tilde{\tau}_1 \tau$  is typically the dominant decay mode of the second lightest neutralino. In  $\chi_1^\pm \chi_2^0$  production we therefore expect three  $\tau$  leptons: one directly from the  $\chi_2^0$  decay and the other from the  $\tilde{\tau}_1$  decays. So in combined  $\chi_1^+ \chi_1^- / \chi_1^\pm \chi_2^0$  production, the expectation is that there will be a significant number of events with two and three  $\tau$  leptons.  $\tau$  leptons are identified by their hadronic decays to thin jets; thus we are interested in the probabilities for obtaining final states with particular numbers of  $\tau$ -jets.

This analysis is performed in the context of the Main Injector (MI) and TeV33 upgrades of the Tevatron collider. The center of mass energy is taken to be  $\sqrt{s} = 2 \text{ TeV}$  and the integrated luminosity is taken to be  $2 \text{ fb}^{-1}$  for the MI upgrade and  $30 \text{ fb}^{-1}$  for the TeV33 upgrade [12].

In performing this analysis, the cuts employed are that final state charged leptons must have  $p_T > 10 \text{ GeV}$  and a pseudorapidity,  $\eta \equiv -\ln(\tan \frac{\theta}{2})$  (where  $\theta$  is the polar angle with respect to the proton beam direction), of magnitude less than 1. Jets must have  $E_T > 10 \text{ GeV}$  and  $|\eta| < 2$ . In addition, hadronic final states within a cone size of  $\Delta R \equiv \sqrt{(\Delta\phi)^2 + (\Delta\eta)^2} = 0.4$  are merged to a single jet. Leptons within this cone radius of a jet are discounted. For a  $\tau$ -jet to be counted as such, it must have  $|\eta| < 1$ . The most energetic  $\tau$  jet is required to have  $E_T > 20 \text{ GeV}$ . In addition, a missing transverse energy cut of  $\cancel{E}_T > 30 \text{ GeV}$  is imposed.

We consider each mass case in turn. In our analysis, we restrict ourselves to those regions of the parameter space where the  $\tilde{\tau}_1$  decays promptly to a  $\tau$  and a gravitino. The parameter space is also restricted to those regions where  $m_{\tilde{\tau}_1} \gtrsim 70 \text{ GeV}$ . Ongoing LEP II analyses

are expected to establish this bound soon [13]. With this restriction, we did not find any examples for Cases 3 and 4.

$$\mathbf{A. Case 1: } m_{\tilde{\nu}} > M_{\chi_2^0} \approx M_{\chi_1^\pm} > m_{\tilde{e}_1, \tilde{\mu}_1} > M_{\chi_1^0} > m_{\tilde{\tau}_1}$$

We consider three examples of this case; the masses and branching ratios of which are given in Table I. We first consider Example 1 which has  $\tan\beta = 20$ ,  $\Lambda = 32$  TeV,  $M = 480$  TeV, and  $n = 2$ . Chargino pair production is particularly simple for this case as  $\chi_1^\pm \rightarrow \tilde{\tau}_1 \nu_\tau$  is not only the dominant decay mode, but is essentially the only decay mode. Thus in chargino pair production, two  $\tau$  leptons are always produced.  $\chi_1^\pm \chi_2^0$  production is almost as simple. The main decay mode of the second heaviest neutralino is  $\chi_2^0 \rightarrow \tilde{\tau}_1 \tau$  with a branching ratio (BR) of 85.3%, while the only other decay modes are  $\chi_2^0 \rightarrow \tilde{e}_1 e$  and  $\chi_2^0 \rightarrow \tilde{\mu}_1 \mu$ . Thus the production probability for three  $\tau$  leptons is high at 85.3% and the three  $\tau$ -jet rate is correspondingly 27.2%.

Example 2 ( $\tan\beta = 34$ ,  $\Lambda = 75$  TeV,  $M = 150$  TeV, and  $n = 1$ ) and Example 3 ( $\tan\beta = 34$ ,  $\Lambda = 85$  TeV,  $M = 340$  TeV, and  $n = 1$ ) are similar.  $\chi_1^\pm \rightarrow \tilde{\tau}_1 \nu_\tau$  is still very much the dominant decay mode, but in these cases  $\chi_1^\pm \rightarrow \chi_1^0 W^\pm$  now occurs with a small but significant BR. On the other hand, the BR for  $\chi_2^0 \rightarrow \tilde{\tau}_1 \tau$  is closer to unity at the expense of  $\chi_2^0 \rightarrow \tilde{e}_1 e$  and  $\chi_2^0 \rightarrow \tilde{\mu}_1 \mu$ .

The question arises as to how high we can expect the  $E_T$  of the  $\tau$ -jets to be. Fig. 1 give the  $E_T$  distribution of the highest  $E_T$   $\tau$ -jet for Example 1. The pseudorapidity cut of  $|\eta| < 1$  on  $\tau$ -jets has been imposed in Fig. 1(b). The peak in the distribution occurs at about 20 GeV with a broad tail that reaches out beyond 120 GeV. Thus the leading  $\tau$ -jets are relatively hard and many will pass the transverse energy cut of  $E_T > 20$  GeV. The next to highest  $E_T$   $\tau$ -jet is significantly different as Fig. 2 shows. Here the distribution peaks at a lower value of about 10 GeV and hardly extends at all above 80 GeV. Due to this softness of the secondary  $\tau$ -jets, many of the  $\tau$ -jets will tend to be eliminated by the cuts. For Example 1, an  $E_T$  cut of 10 GeV on  $\tau$ -jets eliminates about a third of the second highest  $E_T$   $\tau$ -jets in those events with more than 1  $\tau$ -jet.

Also of interest is the  $\cancel{E}_T$  distribution. With energetic and stable gravitinos and neutrinos produced in the decays, it is expected that large missing transverse energy could be an important part of the signal. Since the missing transverse energy is calculated from what is observed, however, the question arises as to whether significant cancellation occurs due to the many decay products. Fig. 3 gives the  $\cancel{E}_T$  distribution for Example 1. The figure demonstrates that the  $\cancel{E}_T$  distribution is indeed broad with a tail reaching out beyond 120 GeV. The peak occurs at about 25 GeV and so a 30 GeV cut should not be too restrictive. Examples 2 and 3 have even harder  $\cancel{E}_T$  distributions since their gaugino masses are larger than for Example 1. Since the  $\cancel{E}_T$  is calculated from what is observable, the spike at  $\cancel{E}_T = 0$  is due to events where none of the jets or charged leptons meet the cuts.

We now consider the specifics of the various final state possibilities. Table II gives the inclusive branching ratios for different numbers of  $\tau$ -jets for Example 1. As indicated above, this example always produces two  $\tau$  leptons in chargino pair production. Before cuts the inclusive branching ratio for the 2  $\tau$ -jet mode in chargino pair production is 41.2%, while the 1  $\tau$ -jet inclusive branching ratio is 45.6%. After the cuts specified above, the branching ratios are cut down rather substantially. The one  $\tau$ -jet BR becomes 22.5% and the two  $\tau$ -jet

BR is 9.0%. Similar results also hold for the other two cases: for Example 2, the branching ratios for which are given in Table III, the before cuts BR for the 2  $\tau$ -jet inclusive BR is 42.0% and the BR for the 1  $\tau$ -jet inclusive BR is 45.0%. There is also a small rate for 3  $\tau$ -jets due to one of the  $\chi_1^\pm$  decaying via the  $\chi_1^\pm \rightarrow \chi_1^0 W^\pm$  mode followed by the decay  $\chi_1^0 \rightarrow \tilde{\tau}_1 \tau$ . The cuts don't eliminate as many of the  $\tau$ -jets for this case as the lightest chargino is more massive than for Example 1. After cuts the two  $\tau$ -jet inclusive BR is 13% and the one  $\tau$ -jet inclusive BR is 29%. Similar results hold for Example 3, see Table IV.

$\chi_1^\pm \chi_2^0$  production most frequently produces 3  $\tau$  leptons and thus there is the possibility of having 3  $\tau$ -jets in these events. For Example 1, the BR before cuts for 3  $\tau$ -jets is 27.2%, while after cuts this goes down to 3.6%. The probability for 2  $\tau$ -jets here is larger than for chargino pair production: before cuts the BR is 44.4% and after cuts the BR is 17.3%. As in the chargino pair case, the reduction after cuts for Examples 2 and 3 is less. For example 2, the inclusive 3  $\tau$ -jet BR before cuts is 27.6% and after the cuts it is 5.7%.

The question now arises as to the observability of these modes at Tevatron's Run II. For Example 1, Table II indicates that the inclusive 3  $\tau$ -jet rate for combined  $\chi_1^+ \chi_1^-$  and  $\chi_1^\pm \chi_2^0$  production is 9.6 fb. For an integrated luminosity of  $2 \text{ fb}^{-1}$  (approximately what is expected initially during Run II), this corresponds to  $\sim 19$  observable events. For  $30 \text{ fb}^{-1}$ , the number of observable events is  $\sim 288$ . The 2  $\tau$ -jets cross section of 62.8 fb gives  $\sim 126$  events for  $2 \text{ fb}^{-1}$  of data and  $\sim 1880$  events for  $30 \text{ fb}^{-1}$  of data. For Example 2, the numbers are lower due to the large masses of the charginos and neutralinos. For  $2 \text{ fb}^{-1}$  ( $30 \text{ fb}^{-1}$ ) of data, the expected number of events for the 3  $\tau$ -jet mode is about 8 (126), while for the 2  $\tau$ -jet mode the expectation is for 49 (737). The number of observed events will be less depending on the  $\tau$ -jet detection efficiency.

The branching ratios for some of the important individual modes are given in Table V for chargino pair production and Table VI for  $\chi_1^\pm \chi_2^0$  production. The electrons and muons are typically too soft to pass the cuts and thus requiring an  $e$  or  $\mu$  to enhance the signal over background probably will be of little help.

## B. Case 2: $M_{\chi_2^0} \approx M_{\chi_1^\pm} > m_{\tilde{\nu}} > M_{\chi_1^0} > m_{\tilde{e}_1, \tilde{\mu}_1} > m_{\tilde{\tau}_1}$

We consider three examples of this case, the masses of which are given in Table VII and the branching ratios are given in Table VIII. This case is more complicated than the previous one due to the shifting of the sneutrino masses below that of  $\chi_1^\pm$  and  $\chi_2^0$  and also to the shifting of the selectron and smuon masses below the mass of the lightest neutralino. As a consequence, there are now many more decay modes for  $\chi_1^\pm$  and  $\chi_2^0$ . The dominant decay mode of the lightest chargino is still  $\chi_1^\pm \rightarrow \tilde{\tau}_1 \nu_\tau$ , but now the decays to the sneutrinos are also important. In fact, the decay to the sneutrinos can have branching ratios approaching that of the decay to the stau: for Example 5, which has  $\tan \beta = 15$ ,  $M = 400 \text{ TeV}$ ,  $\Lambda = 20 \text{ TeV}$ , and  $n = 4$ , we have  $\text{BR}(\chi_1^\pm \rightarrow \tilde{\tau}_1 \nu_\tau) = 0.279$ , while  $\text{BR}(\chi_1^\pm \rightarrow \tilde{\nu}_\tau \tau) = 0.237$ .

For the second lightest neutralino, the dominant decay mode for these examples is  $\chi_2^0 \rightarrow \tilde{\tau}_1 \tau$ . But, as with the decays of the lightest chargino, here the decays to the sneutrinos are important. The branching ratio for the decays of the  $\chi_2^0$  to the sneutrinos tend to range from 10% to 20% each.

Another important difference in this case from the last one is that  $\tilde{e}_1$  and  $\tilde{\mu}_1$  have a lower mass than the lightest neutralino and therefore can not decay to it. Then the only two-body

decay modes for  $\tilde{e}_1$  and  $\tilde{\mu}_1$  that preserve  $R$ -parity are  $\tilde{e}_1 \rightarrow e\tilde{G}$  and  $\tilde{\mu}_1 \rightarrow \mu\tilde{G}$ . Given the smallness of the coupling involved, there is the possibility that some three-body decays are important. For  $\tilde{e}_1$  these are  $\tilde{e}_1^- \rightarrow e^-\tau^-\tilde{\tau}^+$  and  $\tilde{e}_1^- \rightarrow e^-\tau^+\tilde{\tau}^-$  with corresponding decays for  $\tilde{\mu}_1$ . These three-body decays are dominant for all three examples studied.

We now consider the details of the various final state possibilities. Table IX gives the inclusive branching ratios for different numbers of  $\tau$ -jets for Example 4. Given the multitude of decay possibilities presented in Table VIII, up to six  $\tau$  leptons can be produced in  $\chi_1^+\chi_1^-$  events. Moreover, virtually all events produce  $\tau$  leptons since the  $\tilde{e}_1 \rightarrow e\tilde{G}$  and  $\tilde{\mu}_1 \rightarrow \mu\tilde{G}$  decays have nearly negligible branching ratios at the expense of the  $\tau$  producing three-body modes. Before cuts the inclusive branching ratio for the three  $\tau$ -jet mode in chargino pair production is 29.0%, for the two  $\tau$ -jet mode it's 33.8%, and for the one  $\tau$ -jet mode it's 18.0%. After the cuts the branching ratios are cut down rather substantially. The 1  $\tau$ -jet BR becomes 25.9%, the 2  $\tau$ -jet BR is 17.0%, and the 3  $\tau$ -jet BR is 3.7%. Similar results also hold for the other two cases: for Example 5, the branching ratios of which are given in Table X, the one, two, and three  $\tau$ -jet inclusive branching ratios after cuts are 18.7%, 15.2%, and 4.8%, respectively. Similar results also hold for Example 6 as shown in Table XI.

In principle, up to seven  $\tau$  leptons can be produced in  $\chi_1^\pm\chi_2^0$  events albeit the seven  $\tau$  branching ratio is negligible. The main modes of interest are still the one, two, and three  $\tau$ -jet modes. The branching ratios are larger after cuts for these modes than in the chargino pair case, but the values are similar. For Example 4, the branching ratios before cuts for 3  $\tau$ -jets is 33.4%, while after cuts this is substantially reduced to 5.1%. For 2  $\tau$ -jets, the BR before cuts for 2  $\tau$ -jets is 33.4%, while after cuts it is 19.7%.

The  $E_T$  distribution of the lead  $\tau$ -jet for Example 4 is given in Fig. 4 and the  $E_T$  distribution for the secondary  $\tau$ -jet is given in Fig. 5. The distribution for the leading  $\tau$ -jet is quite similar to that of Example 1, but the distribution for the secondary  $\tau$ -jet is somewhat softer due to the decrease in the direct production of  $\tau$  leptons from chargino and neutralino decays and more of the  $\tau$  leptons coming from decays further down the decay chain. The  $\cancel{E}_T$  distribution of the events are shown in Fig. 6.

What is the probability of observing these events at Tevatron Run II or III? For Example 5, the rate for inclusive production of 3  $\tau$ -jets is 8.3 fb. This corresponds to  $\sim 16$  events for an integrated luminosity of  $2\text{ fb}^{-1}$  and  $\sim 249$  events for  $30\text{ fb}^{-1}$ . The inclusive 2  $\tau$ -jet rate is 26.2 fb giving  $\sim 52$  and  $\sim 786$  events for  $2\text{ fb}^{-1}$  and  $30\text{ fb}^{-1}$  of data, respectively. The values for Example 4 are lower due to the larger chargino and neutralino masses. The inclusive 3  $\tau$ -jet cross section is 2.2 fb and the inclusive 2  $\tau$ -jet cross section is 9.1 fb. This gives about 4 (66) and 18 (273) events, respectively.

#### IV. CONCLUSION

We have considered the phenomenology of GMSB models where the lighter stau is the NLSP and decays within the detector. For this situation, the dominant SUSY production processes at the Tevatron are  $\chi_1^+\chi_1^-$  and  $\chi_1^\pm\chi_2^0$ . Their prompt decays lead to events containing  $2\tau$  or  $3\tau$  with high  $p_T$  plus large missing transverse energy. These signals are different from the photonic signals that have been investigated in GMSB models and the dilepton and trilepton signals in the usual supergravity models. Searching for the  $\tau$  lepton signals by the hadronic decays of the  $\tau$  leptons to thin jets is complicated by the fact that, while primary

$\tau$ -jets can have quite high  $E_T$ , the secondary  $\tau$ -jets tend to be rather soft. As a result, many of the  $\tau$ -jets tend to be eliminated by the cuts. Our detailed calculations show that the most promising channel is the inclusive 2  $\tau$ -jets channel, although the production of 3  $\tau$ -jets can be important at the higher integrated luminosity expected at Run III. The missing transverse energy associated with the events is quite large providing a good trigger for these events. Good  $\tau$  identification will be extremely important to detect the signal as well as a detailed understanding of the associated background.

## ACKNOWLEDGMENTS

We thank the members of the GMSB SUSY Run II working group, especially S. Martin and X. Tata for useful communications. Two of us (B. D. and S. N.) also thank the Fermilab Theoretical Physics Department, especially C. T. Hill and J. Lykken for their warm hospitality and support during our summer visit when this work was completed. This work was supported by DOE grant numbers DE-FG06-854ER-40224, DE-FG02-94ER 40852 and DE-FG03-98ER41076.



## REFERENCES

- [1] M. Chertok for the CDF and D0 Collaborations, talk presented at the 33rd Recontres de Moriond: QCD and High Energy Hadronic Interactions, Les Arcs, France, March 21-28, 1998, FERMILAB-Conf-98/156-E; S. Abachi *et al.*, D0 Collaboration, Phys. Rev. Lett. **80**, 442 (1998).
- [2] R. Barate *et al.*, ALEPH Collaboration, Phys. Lett. B **420**, 127 (1998); M. Acciarri *et al.*, L3 Collaboration, CERN-PPE/97-130; K. Ackerstaff *et al.*, OPAL Collaboration, Eur. Phys. J. **C1**, 21 (1998); P. Abreu *et al.*, DELPHI Collaboration, Eur. Phys. J. **C1**, 1 (1998).
- [3] S. Park, representing the CDF collaboration, “Search for New Phenomena in CDF” in *10th Topical Workshop on Proton-Antiproton Collider Physics*, edited by R. Raja and J. Yoh (AIP Press, New York, 1995), report FERMILAB-CONF-95/155-E; R. Culbertson for the CDF and D0 collaborations, talk presented at the 5th International Conference on Supersymmetries in Physics (SUSY 97), Philepdelphia, PA, May 27-31, 1997, FERMILAB-Conf-97/227/E.
- [4] M. Dine and A. Nelson, Phys. Rev. D **47**, 1277 (1993); M. Dine, A. Nelson and Y. Shirman, Phys. Rev. D **51**, 1362 (1995); M. Dine, A. Nelson, Y. Nir and Y. Shirman, Phys. Rev. D **53**, 2658 (1996); M. Dine, Y. Nir and Y. Shirman, Phys. Rev. D **55**, 1501 (1997).
- [5] I. Affleck, M. Dine and N. Seiberg, Nucl. Phys. **B256**, 557 (1997); R. N. Mohapatra and S. Nandi, Phys. Rev. Lett. **79**, 181 (1997); B. Dobrescu, Phys. Lett. B **403**, 285, (1997); Z. Chacko, B. Dutta, R. N. Mohapatra and S. Nandi, Phys. Rev. D **56**, 5466 (1997).
- [6] G.F. Giudice and R. Rattazzi, hep-ph/9801271; S. Dimopoulos, S. Thomas and J. D. Wells, Nucl. Phys. **B488**, 39 (1997); J. Bagger, D. Pierce, K. Matchev and R.-J. Zhang, Phys. Rev. D **55**, 3188 (1997); K. S. Babu, C. Kolda and F. Wilczek, Phys. Rev. Lett. **77**, 3070 (1996); S. Ambrosanio, G. L. Kane, G. D. Kribs, S. P. Martin and S. Mrenna, Phys. Rev. D **54**, 5395 (1996); *ibid.*, Phys. Rev. D **55**, 1372 (1997); H. Baer, M. Brhlik, C.-H. Chen and X. Tata, Phys. Rev. D **56**, 4463 (1997); D. A. Dicus, B. Dutta and S. Nandi, Phys. Rev. Lett. **78**, 3055 (1997); Phys. Rev. D **56**, 5748, (1997); K. Cheung, D. A. Dicus, B. Dutta and S. Nandi, hep-ph/9711216; A. Riotto, O. Tornkvist and R. N. Mohapatra, Phys. Lett. **B388**, 599 (1996); G. Bhattacharyya, A. Romanino, Phys. Rev. D **55**, 7015 (1997); A. Datta, A. Kundu, B. Mukhopadhyaya and S. Roy, Phys. Lett. **B416**, 117 (1998); Y. Nomura, K. Tobe, hep-ph/9708377, S. Raby and K. Tobe, 9805317; S. Raby, hep-ph/9712254; S. P. Martin and J. D. Wells, hep-ph/9805289.
- [7] S. Dimopoulos, M. Dine, S. Raby and S. Thomas, Phys. Rev. Lett. **76**, 3494 (1996); S. Ambrosanio, G. L. Kane, G. D. Kribs, S. P. Martin and S. Mrenna, Phys. Rev. Lett. **76**, 3498 (1996); D. R. Stump, M. Wiest and C.P. Yuan, Phys. Rev. D **54**, 1936 (1996).
- [8] B. Dutta and S. Nandi, hep-ph/9709511; J. L. Feng and T. Moroi, hep-ph/9712499.
- [9] N. G. Deshpande, B. Dutta and S. Oh, Phys. Rev. D **56** 519 (1997); R. Rattazzi and U. Sarid, hep-ph/9612464.
- [10] S. Dimopoulos, G. F. Giudice and A. Pomarol, Phys. Lett. B **389**, 37 (1996); S. P. Martin, Phys. Rev. D **55**, 3177 (1997).
- [11] V. Barger, M. S. Berger, and P. Ohmann, Phys. Rev. D **49**, 4908 (1994).

- [12] P. P. Bagley *et al.*, in *Proceedings of the 1996 DPF/DPB Summer Study on New Directions for High Energy Physics (Snowmass '96)*, Snowmass, CO, June 25-July 12, 1996; D. Amidei *et al.*, unpublished TeV33 Committee report, available at <http://www-theory.fnal.gov/tev33.ps>.
- [13] A. Galloni, DELPHI Collaboration, Talk at “The pheno-CTEQ Symposium 98-Frontiers of Phenomenology”, Madison, Wisconsin March 23-26, 1998; V. Büscher, ALEPH Collaboration, Talk at Fermilab, July 10, 1998, [http://alephwww.cern.ch/~buescher/w\\_c/talk.ps](http://alephwww.cern.ch/~buescher/w_c/talk.ps).

# TABLES

TABLE I. Masses and branching ratios for the three examples of the case where the ordering of the masses is  $m_{\tilde{\nu}} > M_{\chi_2^0} \approx M_{\chi_1^\pm} > m_{\tilde{e}_1, \tilde{\mu}_1} > M_{\chi_1^0} > m_{\tilde{\tau}_1}$ .

	Example 1	Example 2	Example 3
	$\Lambda = 32 \text{ TeV}$	$\Lambda = 75 \text{ TeV}$	$\Lambda = 85 \text{ TeV}$
	$n = 2, M = 15\Lambda$	$n = 1, M = 2\Lambda$	$n = 1, M = 4\Lambda$
	$\tan \beta = 20$	$\tan \beta = 34$	$\tan \beta = 34$
$m_h \text{ (GeV)}$	114	121	122
$m_{H^\pm}$	303	384	451
$m_A$	292	376	444
$m_{\chi_1^0}$	83	105	115
$m_{\chi_2^0}$	149	195	218
$m_{\chi_3^0}$	-273	-370	-439
$m_{\chi_4^0}$	299	386	451
$m_{\chi_{1,2}^\pm}$	148, 300	194, 388	218, 453
$m_{\tilde{\tau}_{1,2}}$	70, 186	95, 287	113, 323
$m_{\tilde{e}_{1,2}}$	92, 178	137, 276	156, 313
$m_{\tilde{\nu}_\tau}$	158	261	300
$m_{\tilde{\nu}_e}$	159	264	303
$m_{\tilde{t}_{1,2}}$	499, 596	794, 883	864, 967
$m_{\tilde{b}_{1,2}}$	528, 574	818, 885	901, 974
$m_{\tilde{u}_{1,2}}$	558, 577	870, 903	962, 1000
$m_{\tilde{d}_{1,2}}$	557, 582	867, 906	959, 1004
$m_{\tilde{g}}$	559	676	737
$\mu$	-264	-363	-433
$\chi_1^\pm \rightarrow \tilde{\tau}_1 \nu_\tau$	1	0.983	0.972
$\chi_1^\pm \rightarrow \chi_1^0 W^\pm$	-	0.017	0.028
$\chi_2^0 \rightarrow \tilde{\tau}_1 \tau$	0.853	0.973	0.978
$\chi_2^0 \rightarrow \tilde{e}_1 e$	0.073	0.013	0.008
$\chi_2^0 \rightarrow \chi_1^0 Z$	-	-	0.006
$\tilde{e}_1 \rightarrow \chi_1^0 e$	1	1	1
$\chi_1^0 \rightarrow \tilde{\tau}_1 \tau$	1	1	1
$\sigma_{p\bar{p} \rightarrow \chi_1^+ \chi_1^-} \text{ (fb)}$	189	56.8	32.0
$\sigma_{p\bar{p} \rightarrow \chi_1^\pm \chi_2^0} \text{ (fb)}$	265	73.5	39.6

TABLE II. Inclusive branching ratios and production rates for different numbers of  $\tau$ -jets for the case where  $\tan \beta = 20$ ,  $M = 480$  TeV,  $\Lambda = 32$  TeV, and  $n = 2$ . The cross section is for combined  $\chi_1^+ \chi_1^- / \chi_1^\pm \chi_2^0$  production.

	1 $\tau$ -jet	2 $\tau$ -jets	3 $\tau$ -jets
$\chi_1^+ \chi_1^-$ : w/o cuts	0.4563	0.4120	-
with cuts	0.2249	0.0902	-
$\chi_1^\pm \chi_2^0$ : w/o cuts	0.2406	0.4438	0.2721
with cuts	0.2291	0.1726	0.0363
Cross section (fb)	103.2	62.77	9.61

TABLE III. Inclusive branching ratios and production rates for different numbers of  $\tau$ -jets for the case where  $\tan \beta = 34$ ,  $M = 150$  TeV,  $\Lambda = 75$  TeV, and  $n = 1$ . The cross section is for combined  $\chi_1^+ \chi_1^- / \chi_1^\pm \chi_2^0$  production.

	1 $\tau$ -jet	2 $\tau$ -jets	3 $\tau$ -jets
$\chi_1^+ \chi_1^-$ : w/o cuts	0.4495	0.4197	0.00954
with cuts	0.2946	0.1304	0.0005
$\chi_1^\pm \chi_2^0$ : w/o cuts	0.2376	0.4406	0.2756
with cuts	0.2789	0.2337	0.0568
Cross section (fb)	37.22	24.58	4.20

TABLE IV. Inclusive branching ratios and production rates for different numbers of  $\tau$ -jets for the case where  $\tan \beta = 34$ ,  $M = 340$  TeV,  $\Lambda = 85$  TeV, and  $n = 1$ . The cross section is for combined  $\chi_1^+ \chi_1^- / \chi_1^\pm \chi_2^0$  production.

	1 $\tau$ -jet	2 $\tau$ -jets	3 $\tau$ -jets
$\chi_1^+ \chi_1^-$ : w/o cuts	0.4444	0.4197	0.0159
with cuts	0.3286	0.1465	0.0003
$\chi_1^\pm \chi_2^0$ : w/o cuts	0.2384	0.4395	0.2734
with cuts	0.2979	0.2530	0.0639
Cross section (fb)	22.30	14.70	2.54

TABLE V. Branching ratios for some of the more interesting final state configurations with and without cuts in chargino pair production.

	Example 1		Example 2		Example 3	
	no cuts	cuts	no cuts	cuts	no cuts	cuts
1 $\tau$ -jet	-	0.1303	-	0.1423	-	0.1440
$e/\mu + 1 \tau$ -jet	0.2281	0.0245	0.2210	0.0400	0.2160	0.0483
1 jet + 1 $\tau$ -jet	-	0.0457	-	0.0651	-	0.0738
2 $\tau$ -jets	0.4200	0.0902	0.4055	0.1265	0.3962	0.1398

TABLE VI. Branching ratios for some of the more interesting final state configurations with and without cuts in  $\chi_1^\pm \chi_2^0$  production.

	Example 1		Example 2		Example 3	
	no cuts	cuts	no cuts	cuts	no cuts	cuts
1 $\tau$ -jet	-	0.0641	-	0.0620	-	0.0572
$e/\mu + \tau$ -jet	-	0.0294	-	0.0364	-	0.0391
2 $e/2 \mu + \tau$ -jet	0.0513	0.0051	0.0575	0.0064	0.0578	0.0074
$e + \mu + \tau$ -jet	0.1026	0.0069	0.1146	0.0011	0.1151	0.0137
2 $\tau$ -jets	-	0.0902	-	0.1106	-	0.1119
1 jet + 2 $\tau$ -jets	-	0.0328	-	0.0536	-	0.0593
$e/\mu + 2 \tau$ -jets	0.1894	0.0219	0.2119	0.0319	0.2113	0.0378
3 $\tau$ -jets	0.2322	0.0344	0.2622	0.0556	0.2573	0.0625

TABLE VII. Masses and branching ratios for the three examples of the case where the ordering of the masses is  $M_{\chi_2^0} \approx M_{\chi_1^\pm} > m_{\tilde{\nu}} > M_{\chi_1^0} > m_{\tilde{e}_1, \tilde{\mu}_1} > m_{\tilde{\tau}_1}$ .

	Example 4	Example 5	Example 6
	$\Lambda = 32 \text{ TeV}$	$\Lambda = 20 \text{ TeV}$	$\Lambda = 22 \text{ TeV}$
	$n = 3, M = 4.69\Lambda$	$n = 4, M = 20\Lambda$	$n = 4, M = 40\Lambda$
	$\tan \beta = 12$	$\tan \beta = 15$	$\tan \beta = 18$
$m_h \text{ (GeV)}$	118	115	117
$m_{H^\pm}$	373	301	339
$m_A$	364	290	329
$m_{\chi_1^0}$	127	104	116
$m_{\chi_2^0}$	224	180	206
$m_{\chi_3^0}$	-316	-268	-308
$m_{\chi_4^0}$	355	307	341
$m_{\chi_{1,2}^\pm}$	222, 355	178, 307	205, 341
$m_{\tilde{\tau}_{1,2}}$	101, 220	71, 174	73, 194
$m_{\tilde{e}_{1,2}}$	108, 218	86, 168	94, 186
$m_{\tilde{\nu}_\tau}$	202	147	168
$m_{\tilde{\nu}_e}$	202	147	168
$m_{\tilde{t}_{1,2}}$	658, 764	500, 611	544, 663
$m_{\tilde{b}_{1,2}}$	710, 735	541, 575	591, 633
$m_{\tilde{u}_{1,2}}$	726, 748	562, 578	619, 637
$m_{\tilde{d}_{1,2}}$	725, 752	562, 584	619, 642
$m_{\tilde{g}}$	826	690	755
$\mu$	-310	-260	-301
$\sigma_{p\bar{p} \rightarrow \chi_1^+ \chi_1^-} \text{ (fb)}$	22.9	71.8	37.2
$\sigma_{p\bar{p} \rightarrow \chi_1^\pm \chi_2^0} \text{ (fb)}$	26.3	89.4	45.1

TABLE VIII. Branching ratios for the three examples of the case where the ordering of the masses is  $M_{\chi_2^0} \approx M_{\chi_1^\pm} > m_{\tilde{\nu}} > M_{\chi_1^0} > m_{\tilde{e}, \tilde{\mu}} > m_{\tilde{\tau}_1}$ .

	Example 4	Example 5	Example 6
	$\Lambda = 32 \text{ TeV}$	$\Lambda = 20 \text{ TeV}$	$\Lambda = 22 \text{ TeV}$
	$n = 3, M = 4.69\Lambda$	$n = 4, M = 20\Lambda$	$n = 4, M = 40\Lambda$
	$\tan \beta = 12$	$\tan \beta = 15$	$\tan \beta = 18$
$\chi_1^\pm \rightarrow \tilde{\tau}_1 \nu_\tau$	0.3397	0.2793	0.2905
$\chi_1^\pm \rightarrow \tilde{\nu}_\tau \tau$	0.1895	0.2371	0.2104
$\chi_1^\pm \rightarrow \tilde{\nu}_e e$	0.1777	0.2210	0.1944
$\chi_1^\pm \rightarrow \chi_1^0 W^\pm$	0.1096	-	0.0138
$\chi_1^\pm \rightarrow \tilde{\tau}_2 \nu_\tau$	-	0.0025	0.0111
$\chi_1^\pm \rightarrow \tilde{e}_2 \nu_e$	0.0064	0.0195	0.0427
$\chi_2^0 \rightarrow \tilde{\tau}_1 \tau$	0.3824	0.3513	0.3458
$\chi_2^0 \rightarrow \tilde{e}_1 e$	0.1235	0.0812	0.0398
$\chi_2^0 \rightarrow \tilde{\nu}_\tau \nu_\tau$	0.1091	0.1358	0.1450
$\chi_2^0 \rightarrow \tilde{\nu}_e \nu_e$	0.1066	0.1332	0.1411
$\chi_2^0 \rightarrow \tilde{\tau}_2 \tau$	0.0045	0.0096	0.0212
$\chi_2^0 \rightarrow \tilde{e}_2 e$	0.0141	0.0373	0.0632
$\chi_2^0 \rightarrow \chi_1^0 Z$	0.0158	-	-
$\chi_1^0 \rightarrow \tilde{\tau}_1 \tau$	0.4573	0.5769	0.6018
$\chi_1^0 \rightarrow \tilde{e}_1 e$	0.2713	0.2115	0.1991
$\tilde{\nu}_\tau \rightarrow \chi_1^0 \nu_\tau$	0.8759	1	0.6775
$\tilde{\nu}_\tau \rightarrow \tilde{\tau}_1 W$	0.1241	-	0.3225
$\tilde{\nu}_e \rightarrow \chi_1^0 \nu_e$	1	1	1
$\tilde{e}_2 \rightarrow \chi_1^0 e$	1	1	1
$\tilde{e}_1 \rightarrow e^- \tau^- \tilde{\tau}_1^+$	0.5874	0.6240	0.6441
$\tilde{e}_1 \rightarrow e^- \tau^+ \tilde{\tau}_1^-$	0.4091	0.3760	0.3559
$\tilde{e}_1 \rightarrow e \tilde{G}$	0.0036	$\sim 10^{-5}$	$\sim 10^{-6}$
$\tilde{\tau}_2 \rightarrow \chi_1^0 \tau$	1	1	1

TABLE IX. Inclusive branching ratios and production rates for different numbers of  $\tau$ -jets for the case where  $\tan \beta = 12$ ,  $M = 150$  TeV,  $\Lambda = 32$  TeV, and  $n = 3$ . The cross section is for combined  $\chi_1^+ \chi_1^- / \chi_1^\pm \chi_2^0$  production.

	1 $\tau$ -jet	2 $\tau$ -jets	3 $\tau$ -jets	4 $\tau$ -jets	5 $\tau$ -jets
$\chi_1^+ \chi_1^-$ : w/o cuts	0.1804	0.3378	0.2897	0.1257	0.0282
with cuts	0.2529	0.1704	0.0367	0.0040	0.0002
$\chi_1^\pm \chi_2^0$ : w/o cuts	0.1464	0.3344	0.3336	0.1399	0.0216
with cuts	0.2687	0.1966	0.0513	0.0048	0.0002
Cross section (fb)	12.86	9.07	2.19	0.22	0.01

TABLE X. Inclusive branching ratios and production rates for different numbers of  $\tau$ -jets for the case where  $\tan \beta = 15$ ,  $M = 400$  TeV,  $\Lambda = 20$  TeV, and  $n = 4$ . The cross section is for combined  $\chi_1^+ \chi_1^- / \chi_1^\pm \chi_2^0$  production.

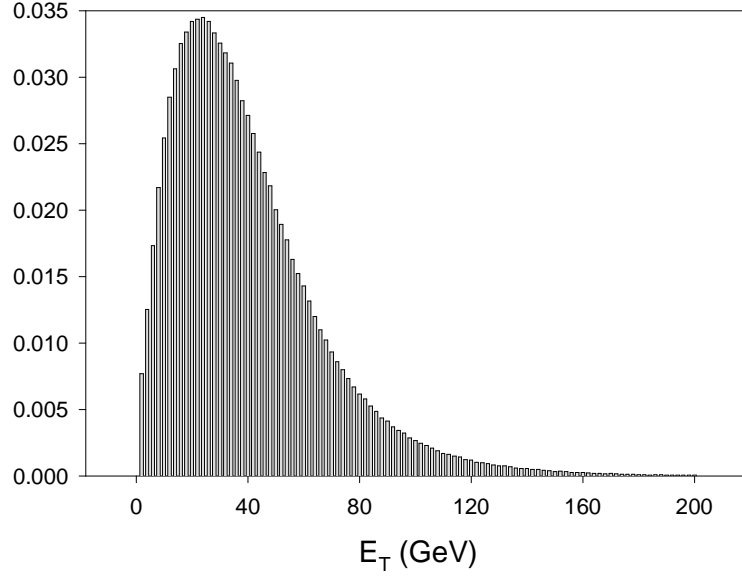
	1 $\tau$ -jet	2 $\tau$ -jets	3 $\tau$ -jets	4 $\tau$ -jets	5 $\tau$ -jets
$\chi_1^+ \chi_1^-$ : w/o cuts	0.1534	0.3138	0.3058	0.1537	0.0414
with cuts	0.1865	0.1522	0.0481	0.0075	0.0005
$\chi_1^\pm \chi_2^0$ : w/o cuts	0.1323	0.3155	0.3391	0.1618	0.0299
with cuts	0.1993	0.1709	0.0544	0.0079	0.0003
Cross section (fb)	31.21	26.21	8.32	1.25	0.07

TABLE XI. Inclusive branching ratios and production rates for different numbers of  $\tau$ -jets for the case where  $\tan \beta = 18$ ,  $M = 880$  TeV,  $\Lambda = 22$  TeV, and  $n = 4$ . The cross section is for combined  $\chi_1^+ \chi_1^- / \chi_1^\pm \chi_2^0$  production.

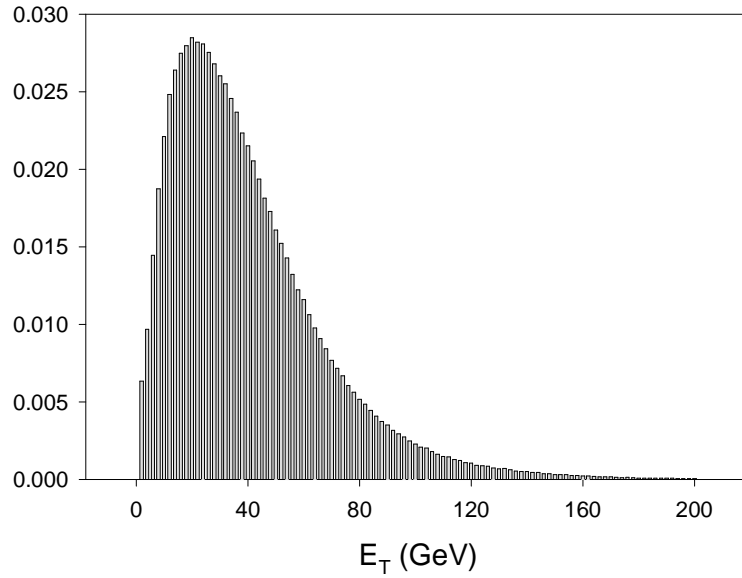
	1 $\tau$ -jet	2 $\tau$ -jets	3 $\tau$ -jets	4 $\tau$ -jets	5 $\tau$ -jets
$\chi_1^+ \chi_1^-$ : w/o cuts	0.1690	0.3354	0.3034	0.1348	0.0252
with cuts	0.2112	0.1821	0.0592	0.0089	0.0004
$\chi_1^\pm \chi_2^0$ : w/o cuts	0.1436	0.3286	0.3360	0.1468	0.0203
with cuts	0.2173	0.1976	0.0675	0.0110	0.0006
Cross section (fb)	17.65	15.68	5.24	0.82	0.04



# FIGURES

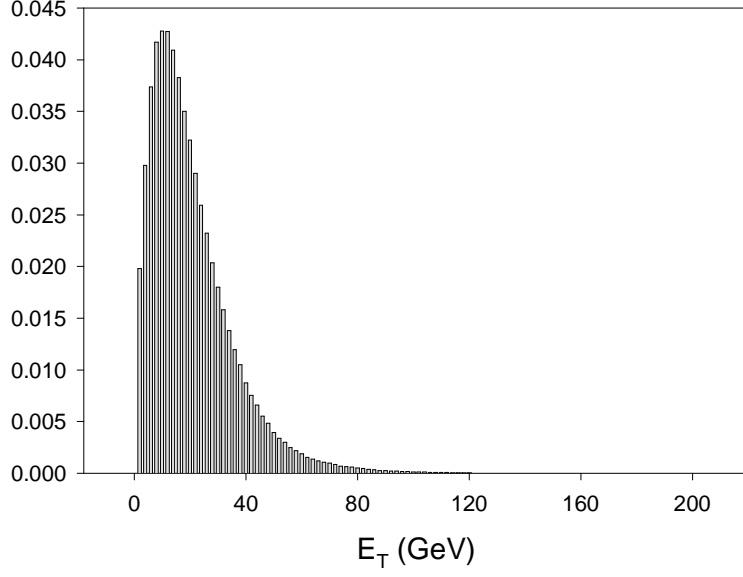


(a)

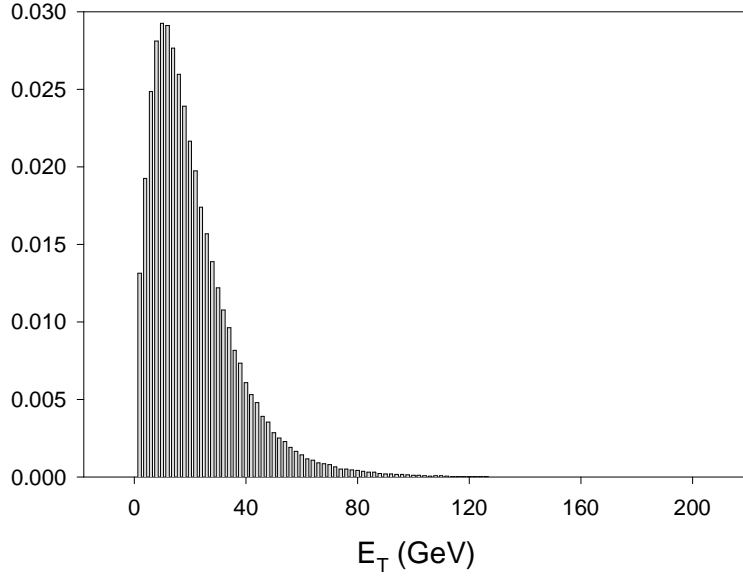


(b)

FIG. 1.  $E_T$  distribution of the highest  $E_T$   $\tau$ -jet in  $\chi_1^+ \chi_1^- / \chi_1^\pm \chi_2^0$  production for Example 1. In (a) no cuts are imposed, while in (b) a pseudorapidity cut of  $|\eta| < 1$  is imposed on the  $\tau$ -jets.

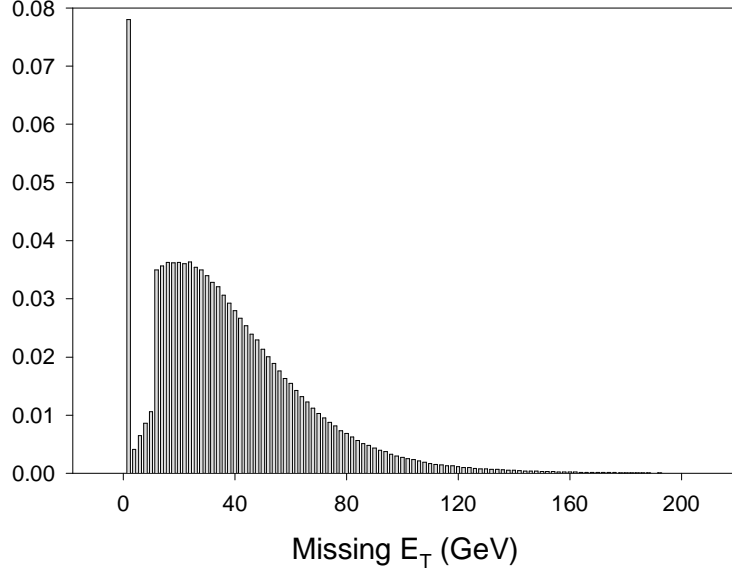


(a)

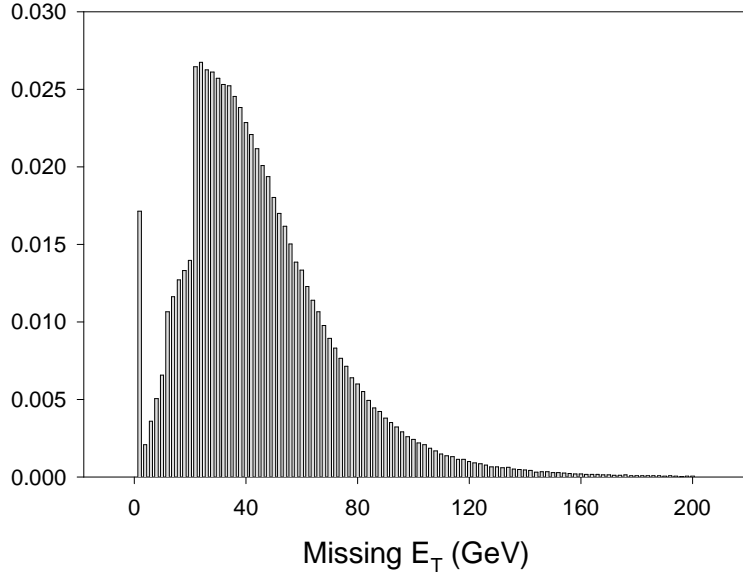


(b)

FIG. 2.  $E_T$  distribution of the next to highest  $E_T$   $\tau$ -jet in  $\chi_1^+ \chi_1^- / \chi_1^\pm \chi_2^0$  production for Example 1. In (a) no cuts are imposed, while in (b) a pseudorapidity cut of  $|\eta| < 1$  is imposed on the  $\tau$ -jets.

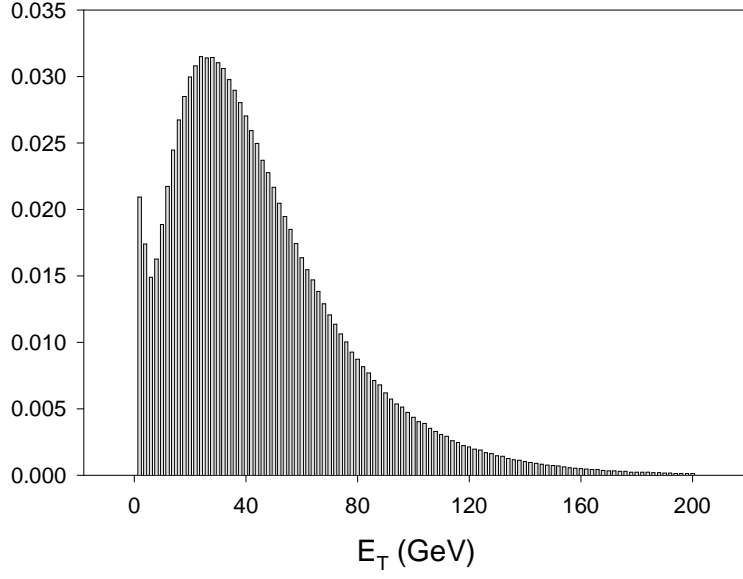


(a)

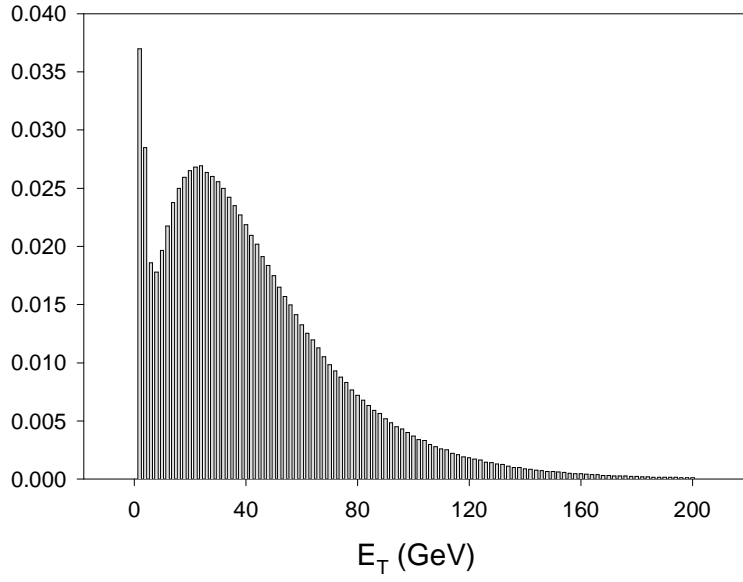


(b)

FIG. 3.  $\cancel{E}_T$  distribution for  $\chi_1^+ \chi_1^- / \chi_1^\pm \chi_2^0$  production for Example 1. In (a) the cuts used are that the jets must satisfy  $E_T > 10$  GeV and  $|\eta| < 2$  ( $|\eta| < 1$  for  $\tau$ -jets), while electrons and muons must satisfy  $p_T > 10$  GeV and  $|\eta| < 1$ . In (b) the cuts are as in (a) except that the highest  $E_T$   $\tau$ -jet must now satisfy  $E_T > 20$  GeV.

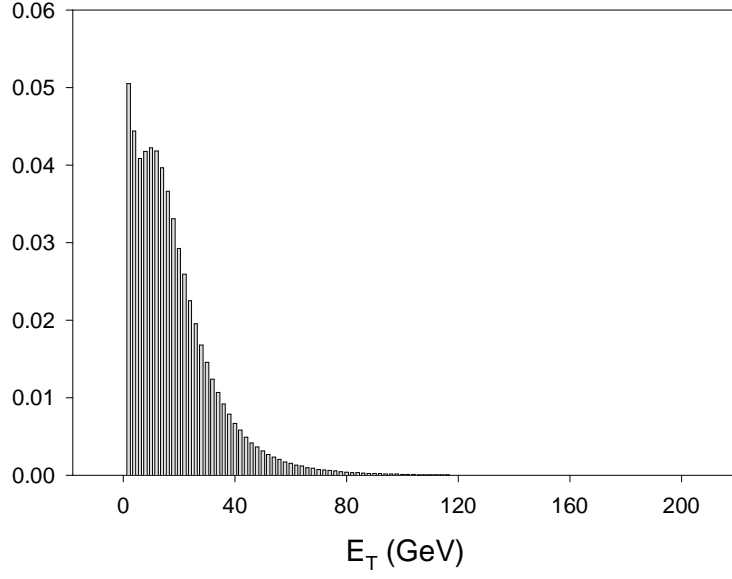


(a)

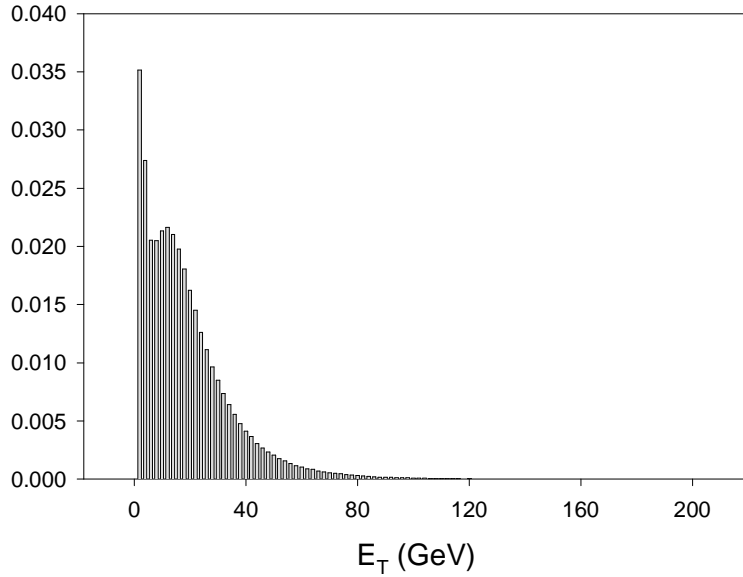


(b)

FIG. 4.  $E_T$  distribution of the highest  $E_T$   $\tau$ -jet in  $\chi_1^+ \chi_1^- / \chi_1^\pm \chi_2^0$  production for Example 4. In (a) no cuts are imposed, while in (b) a pseudorapidity cut of  $|\eta| < 1$  is imposed on the  $\tau$ -jets.

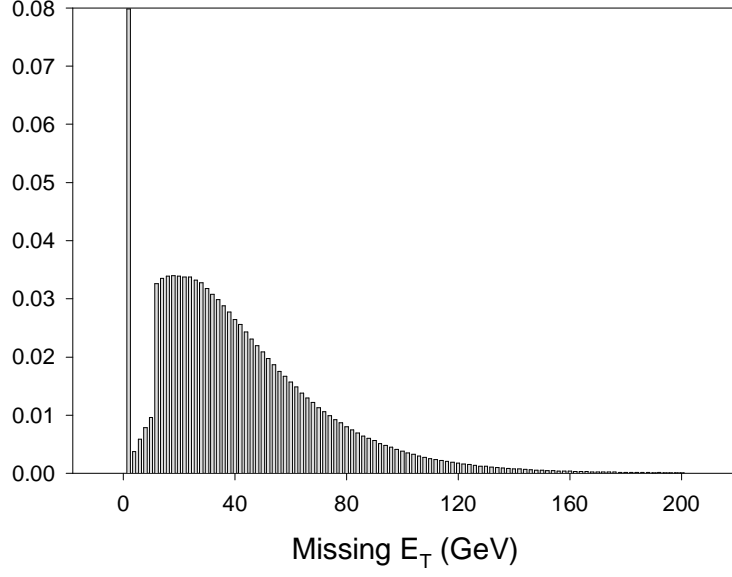


(a)

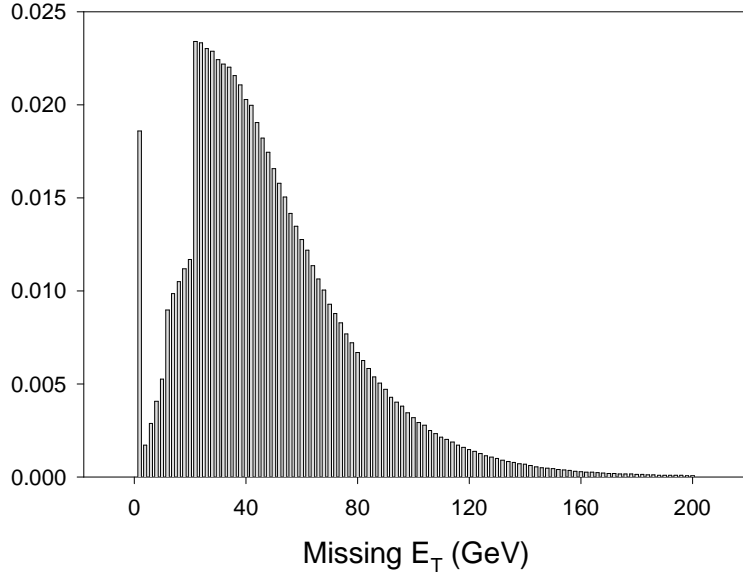


(b)

FIG. 5.  $E_T$  distribution of the next to highest  $E_T$   $\tau$ -jet in  $\chi_1^+ \chi_1^- / \chi_1^\pm \chi_2^0$  production for Example 4. In (a) no cuts are imposed, while in (b) a pseudorapidity cut of  $|\eta| < 1$  is imposed on the  $\tau$ -jets.



(a)



(b)

FIG. 6.  $\cancel{E}_T$  distribution for  $\chi_1^+ \chi_1^- / \chi_1^\pm \chi_2^0$  production for Example 1. In (a) the cuts used are that the jets must satisfy  $E_T > 10$  GeV and  $|\eta| < 2$  ( $|\eta| < 1$  for  $\tau$ -jets), while electrons and muons must satisfy  $p_T > 10$  GeV and  $|\eta| < 1$ . In (b) the cuts are as in (a) except that the highest  $E_T$   $\tau$ -jet must now satisfy  $E_T > 20$  GeV.